ELSEVIER

Materials Science and Engineering A 426 (2006) 305–313

MATERIALS SCIENCE & ENGINEERING A

www.elsevier.com/locate/msea

Effect of equal channel angular pressing on tensile properties and fracture modes of casting Al–Cu alloys

D.R. Fang [a,b], Z.F. Zhang [a,*], S.D. Wu [a], C.X. Huang [a], H. Zhang [a], N.Q. Zhao [b], J.J. Li [b]

[a] *Shenyang National Laboratory for Materials Science, Institute of Metal Research, Chinese Academy of Sciences, 72 Wenhua Road, Shenyang 110016, People's Republic of China*

[b] *School of Materials Science and Engineering, Tianjin University, 92 Weijin Road, Tianjin 300072, People's Republic of China*

Received 23 October 2005; accepted 13 April 2006

Abstract

Tensile strength, elongation, static toughness and fracture modes of casting Al–0.63 wt.% Cu and Al–3.9 wt.% Cu alloys subjected to equal channel angular pressing (ECAP) were investigated. It is found that the grains of the two alloys can be refined to submicron level after four passes of ECAP. In addition, precipitation phase θ along grain boundaries in the Al–3.9 wt.% Cu alloy was also broken after ECAP treatment. The tensile fracture strength increases with increasing ECAP pass for both of the Al–Cu alloys, however, the elongation is almost independent of the ECAP pass. Consequently, the static toughness of the Al–Cu alloys is enhanced at high ECAP pass. The failure modes of Al–0.63 wt.% Cu alloy consist of necking and shear fracture, however, Al–3.9 wt.% Cu alloy displays normal fracture and shear fracture with different shear angle. Based on the results above, the tensile properties and failure modes of the Al–Cu alloys are discussed.

Keywords: Al–Cu alloys; Equal channel angular pressing (ECAP); Tensile strength; Elongation; Static toughness; Fracture modes

1. Introduction

In the past decade, equal channel angular pressing (ECAP) technique has attracted much attention as a method of severe plastic deformation [1–4]. ECAP can apply a high shear strain to materials through a specially designed die having two equally sized channels connected at a finite angle [1,5]. The technique has been proven to be very useful in improving mechanical properties of metals and alloys, leading to high strength or superplasticity, through grain refinement down to submicron level [6–8].

ECAP has been applied to various Al alloys, mainly in Al–Mg alloys [4,6–8], however, there are few reports on Al–Cu alloys processed by ECAP so far. Murayama et al. [9] studied the microstructure of Al–1.7 at% Cu alloy deformed by ECAP. They used the Al–Cu alloy samples through solution treatment and aging, θ' precipitates were almost completely dissolved after eight passes of ECAP, and nearly single-phase microstructure with a fine grain was obtained. Wang et al. [10] applied ECAP to a lamellae Al–33% Cu eutectic alloy, and shear features of the material was investigated. However, the reports about mechanical properties of the ECAPed Al–Cu alloys have not yet been seen.

Al–Cu alloys are a common kind of casting Al-alloys, the microstructure in the casting state consists of aluminium solution with a very heterogeneous distribution of copper and coarse brittle θ phase (Al_2Cu) precipitated along grain boundaries [11]. Because of their poor mechanical properties, usually, Al–Cu alloys are not utilized in casting condition. The traditional process is to make the second-phase precipitate dispersedly by solution treatment and aging in order to strengthen alloys in industry applications [12]. The present research tries to strengthen Al–Cu alloys by ECAP technique, absolutely without any aging treatment. By multi-pass ECAP process to a casting Al–3.9% Cu alloy, we expect that the coarse brittle θ phase can be broken into small particles, and distributes uniformly. Besides, ECAP will probably refine its microstructure and produce a lot of defects. Consequently, the mechanical properties of the Al–Cu alloy can be improved by both dispersion strengthening and refinement of microstructure.

* Corresponding author. Tel.: +86 24 23971043; fax: +86 24 23891320.
E-mail address: zhfzhang@imr.ac.cn (Z.F. Zhang).

0921-5093/$ – see front matter © 2006 Elsevier B.V. All rights reserved.
doi:10.1016/j.msea.2006.04.044

2. Experimental procedure

The experiment materials are casting Al–3.9% Cu and Al–0.63% Cu (in wt.%) alloy ingots. First, these Al–Cu alloy ingots were made into rods of 10 mm in diameter and 80 mm in length by spark cutting technique. Then, equal channel angular pressing (ECAP) was conducted at room temperature using a solid die having an angle of 90° between the two channels. The samples subjected to repetitive pressing were rotated by 90° in the same direction between each pass in the procedure designated route B_C [13]. Early experiments on pure Al showed that the route B_C most expeditiously led to an array of equiaxed grains separated by boundaries having high angles of misorientation [14]. Before pressing, the rods were coated with MoS_2 as lubricant. The numbers of ECAP pass are 1, 2, 4 and 6 for Al–0.63% Cu alloy, and 1, 2 and 4 for Al–3.9% Cu alloy, because it is quite difficult to press Al–3.9% Cu alloy when the ECAP pass is over 4.

After ECAP, tensile specimens with cross-section of 3 mm × 5 mm and gauge length of 14 mm were machined from the ECAPed samples with their tensile axes lying parallel to the pressing direction. The horizontal along the pressing direction was defined as *X* plane, and the vertical was *Y* plane, as shown in Fig. 1. Tensile specimens were mechanically polished and followed by electropolishing in a solution of $HClO_4$ and C_2H_5OH. These specimens were subjected to tensile load upto failure at room temperature using MTS mini testing machine operating at a constant rate of cross-head displacement with a strain rate of about $5 \times 10^{-4}s^{-1}$.

The microstructure observations were performed using a S360 Cambridge scanning electron microscopy (SEM) and a JEM-2000FX II transmission electron microscopy (TEM). The thin foils for TEM observations were cut from the center of the pressed rods parallel to the *Y* plane, mechanically ground to about 50 μm and finally thinned by twin-jet electropolishing method with a solution of 33% nitric acid–methanol.

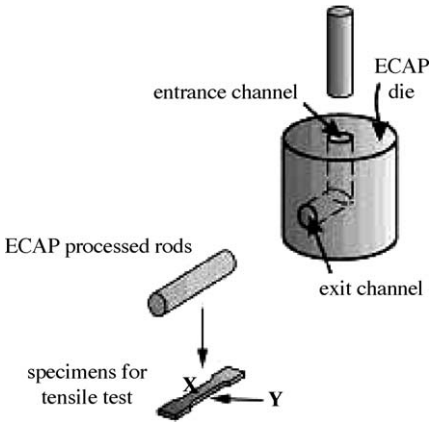

Fig. 1. Machining direction of tensile specimens.

3. Results and discussion

3.1. Microstructures before and after ECAP

Fig. 2(a and b) shows the microstructure of the casting Al–0.63% Cu alloy. It can be seen that there is only few of dot-like θ phase distributing in the matrix, and the average grain size is about 400 μm. For the casting Al–3.9% Cu alloy, the average grain size is about 120 μm. Meanwhile, it is evident that there are more θ phase precipitated along grain boundaries, exhibiting a net-like feature, as shown in Fig. 2(c and d).

Fig. 3 shows the SEM micrograph of the Al–0.63% Cu alloy processed by ECAP. After one or two passes, the microstructure

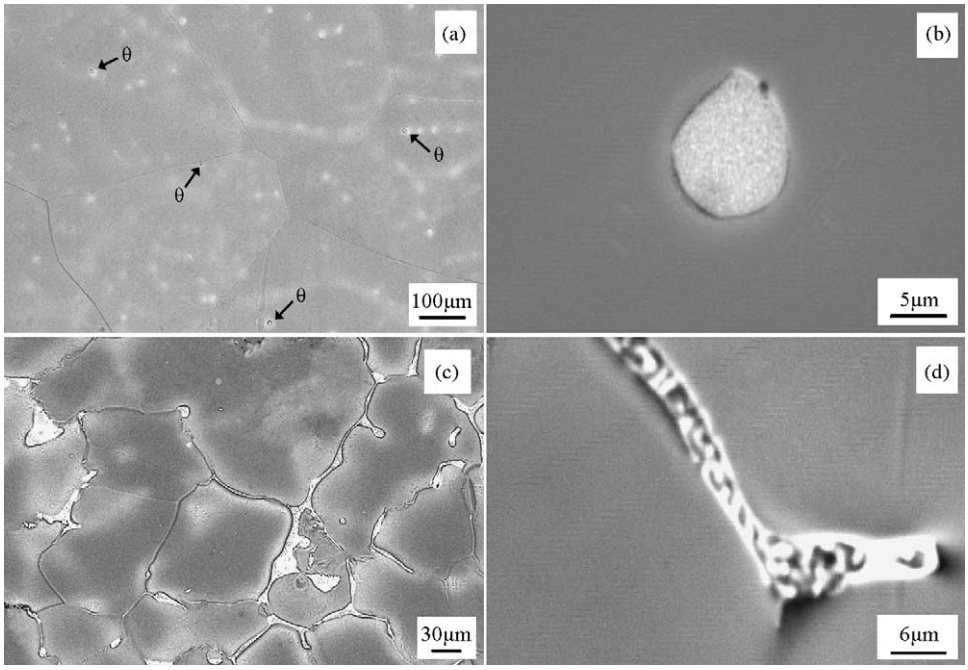

Fig. 2. Microstructures of the two casting Al–Cu alloys: (a and b) Al–0.63% Cu alloy and (c and d) Al–3.9% Cu alloy.

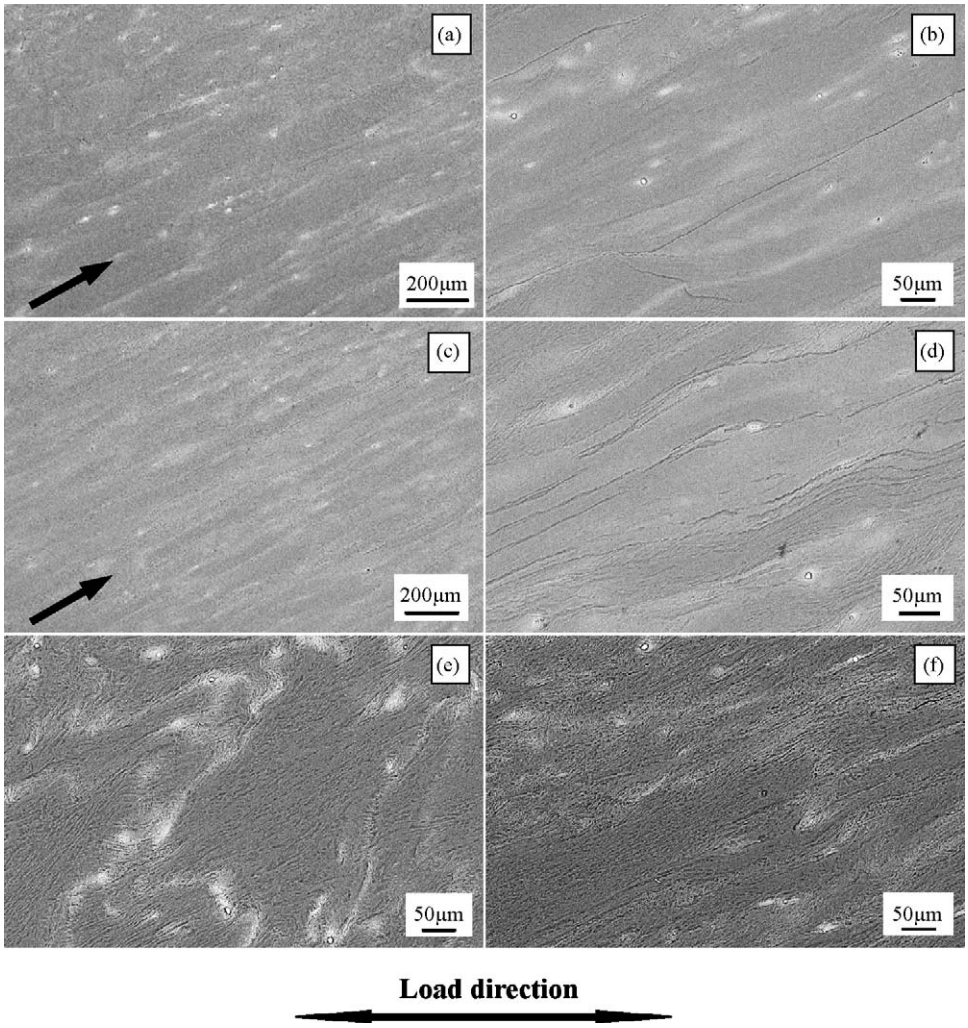

Fig. 3. SEM micrographs of Al–0.63% Cu alloy after different ECAP passes (*Y* plane): (a and b) one pass, (c and d) two passes, (e) four passes and (f) six passes.

of the alloys presents streamline feature along the shear direction, as shown in Fig. 3(a and c). The streamline makes an angle of about 26° with respect to the longitudinal direction, which is well consistent with the previous analysis [15]. It can be seen from Fig. 3(b and d) that the grains were elongated due to severe shear deformation. However, the streamline disappears after four passes, forming a homogeneous microstructure (see Fig. 3(e)), and the elongated grains were seen again after six passes (see Fig. 3(f)).

Fig. 4 is the SEM micrograph of the Al–3.9% Cu alloy processed by ECAP. After one pass, the net-like θ phase was broken due to strong shear process, as shown in Fig. 4(a and b). After two passes, the θ phase was further broken along the shear direction (see Fig. 4(c and d)). In the same way, the grains were elongated after one or two passes. After four passes, the shear streamline disappears, as that in Al–0.63% Cu alloy, indicating that the θ phase has almost been broken into disperse particles, as shown in Fig. 4(e and f).

The microstructure of Al–0.63% Cu alloy observed by TEM is shown in Fig. 5(a). It is apparent that its grains have been refined to submicron level after four passes of ECAP. For Al–3.9% Cu alloy, similar grain refinement can also be achieved after four passes, forming a microstructure with gain size of about 200–300 nm, as seen in Fig. 5(b). In addition, the distribution of the θ phase in Al–3.9% Cu alloy can be seen more clearly in Fig. 5(c and d). It is noted that some θ particles have been refined to nanoscale, as clearly seen in Fig. 5(d) by enlarging the microstructure in the dashed frame in Fig. 5(c).

The streamline produced by ECAP was mentioned in the research of Gholinia et al. [16], who described the shear deformation in terms of streamline coordinates. In addition, Furuno et al. [17] applied ECAP to pure Al, and the microstructures also contain streamline after ECAP. Above mentioned shearing patterns during ECAP were discussed by Furukawa et al. [3] and Gholinia et al. [18]. Fig. 6 illustrates concisely the forming and disappearing of the streamline patterns during ECAP by route B_C. If considering a small sample unit with rectangular shape on the *Y* plane, the evolution of streamline patterns will be the processes in Fig. 6(a and b), forming a tilted parallelogram. Then the sample was rotated for 90°, and the parallelogram also turn around to the *X* plane. It is supposed that the parallelogram slice is so small that it only moves when pressed, without shape change. After second pass, the sample was rotated for 90° again, and the parallelogram comes back to the *Y* plane, but its shape

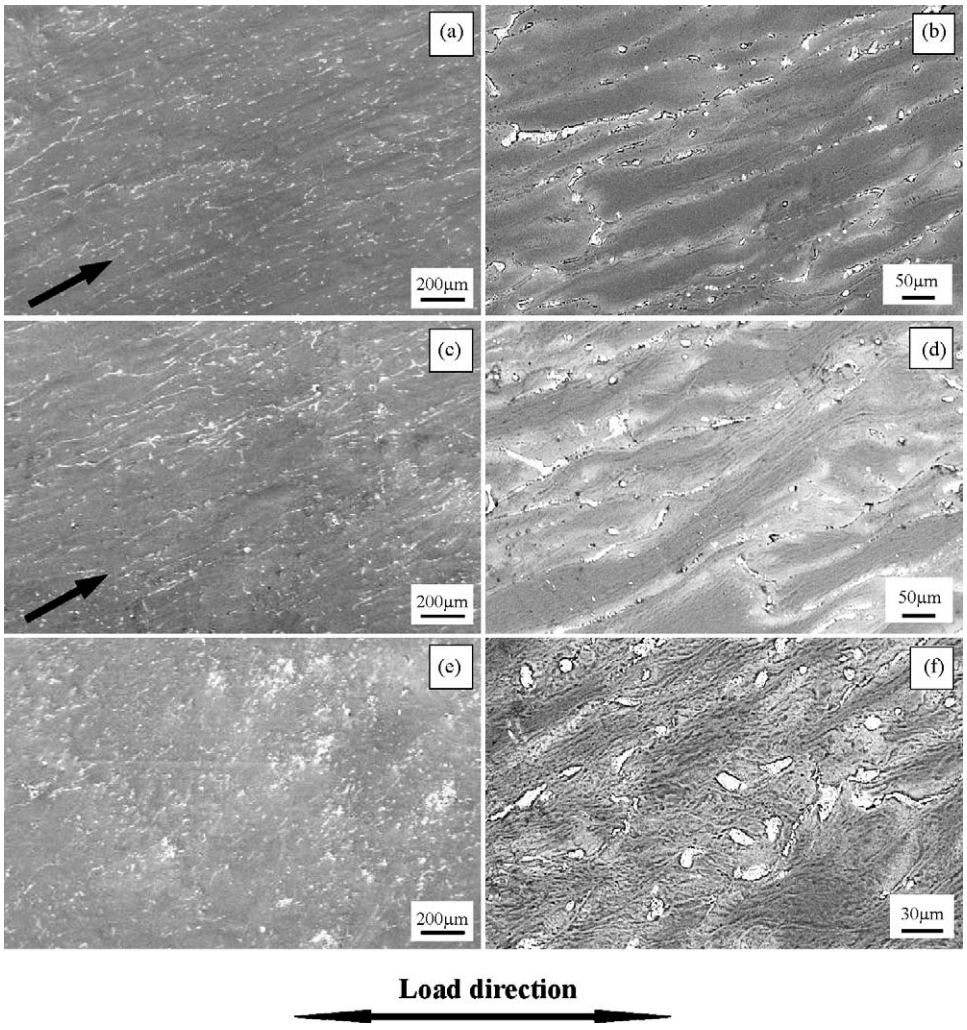

Fig. 4. SEM micrographs of Al–3.9% Cu alloy after different ECAP passes (*Y* plane): (a and b) one pass, (c and d) two passes and (e and f) four passes.

is reversed in comparison with the initial parallelogram. Thus, after third pass, the tilted parallelogram was pressed to rectangular again, leading to the disappearance of the streamline patterns, as illustrated in Fig. 6(c and d) and the observations in Figs.3(e) and 4(e).

3.2. Tensile properties

3.2.1. Effect of ECAP on strength and elongation

The tensile properties of the two Al–Cu alloys are shown in Figs. 7 and 8. It demonstrates that the elongation of the Al–0.63% Cu alloy is better than that of the Al–3.9% Cu alloy, while the strength of Al–3.9% Cu is obviously higher than that of Al–0.63% Cu.

The strength of Al–0.63% Cu alloy increases clearly with increasing ECAP passes, as a result of work-hardening. Its ultimate tensile strength (UTS) is increased from 83 to 239 MPa after six passes. However, its elongation decreases drastically after one pass, from 47.8 to 19.4%. Then its elongation almost maintains constant, independent of ECAP pass. The variation of strength and elongation for Al–0.63% Cu alloy processed by ECAP is consistent with some Al–Mg alloys [19]. It can be seen from Fig. 7(a) that the UTS of the ECAPed Al–0.63% Cu samples reaches after rapid strain hardening, followed by an extensive strain softening, while the strain hardening capacity of the casting sample is higher than the ECAPed samples.

For Al–3.9% Cu alloy, the strength and elongation show the similar trend with those of Al–0.63% Cu alloy during ECAP treatment. Its UTS is 207 MPa after one pass, and reaches 290 MPa after four passes. However, the elongation decreases drastically after one pass, from 7.8 to 1.5%. Thereafter, the elongation increases slightly with increasing ECAP passes, and reaches 2.7% after four passes. The similar variation of the tensile properties above was also observed in AlMgSi alloy [20] and 2024 Al alloy [21] processed by ECAP. For Al–3.9% Cu alloy, the strengthening effect can be attributed to two factors, i.e. grain refinement and the dispersion of the broken θ phase. Mechanical properties of aged Al–4.5 wt.% Cu alloy were studied in the reference [11], its UTS is 220 MPa and elongation is 8.6%. From the data above, multi-passed Al–3.9% Cu alloy is better than aged Al–Cu alloy in strength but worse in elongation.

The strain-hardening exponent n was calculated according to the tensile stress–strain curves of the two Al–Cu alloys, and are listed in Table 1. It can be seen that the strain-hardening exponent

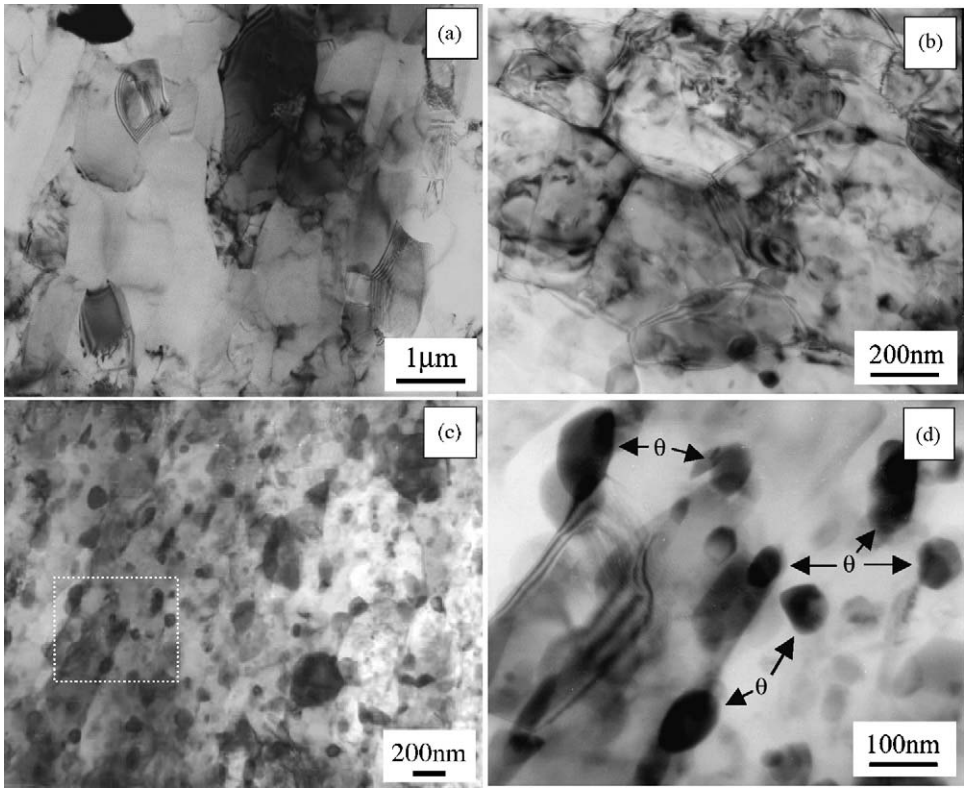

Fig. 5. TEM micrographs of Al–Cu alloys after four passes of ECAP observed on *Y* plane: (a) Al–0.63% Cu alloy and (b–d) Al–3.9% Cu alloy.

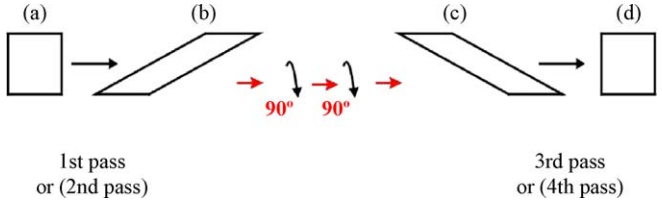

Fig. 6. Evolution of the streamline patterns with different ECAP passes for B_C route.

n of the Al–0.63% Cu alloys is about 0.34–0.39 except for the sample after two passes of ECAP. However, for the Al–3.9% Cu alloy, its strain-hardening exponent *n* is almost constant of 0.42–0.43 after ECAP.

Table 1
Strain-hardening exponent of the two Al–Cu alloys after ECAP

	As-cast	One pass	Two passes	Four passes	Six passes
Al–0.63% Cu	0.38	0.34	0.23	0.38	0.39
Al–3.9% Cu	0.29	0.43	0.43	0.42	

3.2.2. *Effect of ECAP on static toughness*

Static toughness represents comprehensive mechanical property of materials, and claims good coordination of materials' strength and plasticity. The static toughness *U* of materials can be calculated by [22]

$$U = \int_0^{\varepsilon_f} \sigma \mathrm{d}\,\varepsilon,$$

where σ is flow stress, ε_f is total strain at fracture. Ye and Wang [23] proposed static toughness for characterizing comprehensively the variation of the static mechanical property parameters for 45# medium carbon structural steel during fatigue failure

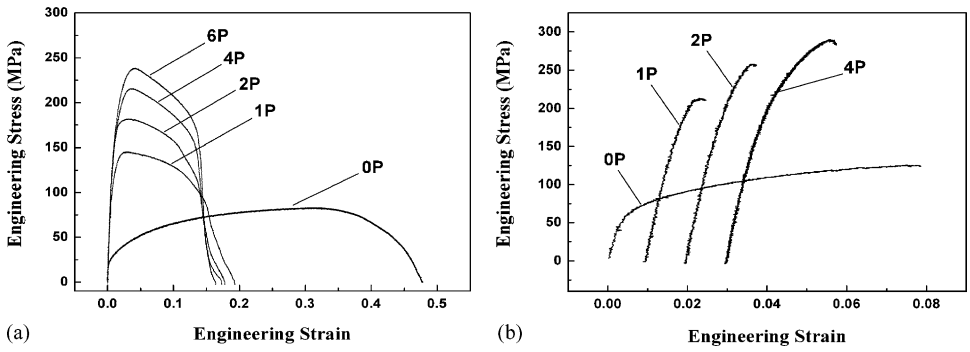

Fig. 7. Tensile stress–strain curves of: (a) Al–0.63% Cu alloy and (b) Al–3.9% Cu alloy.

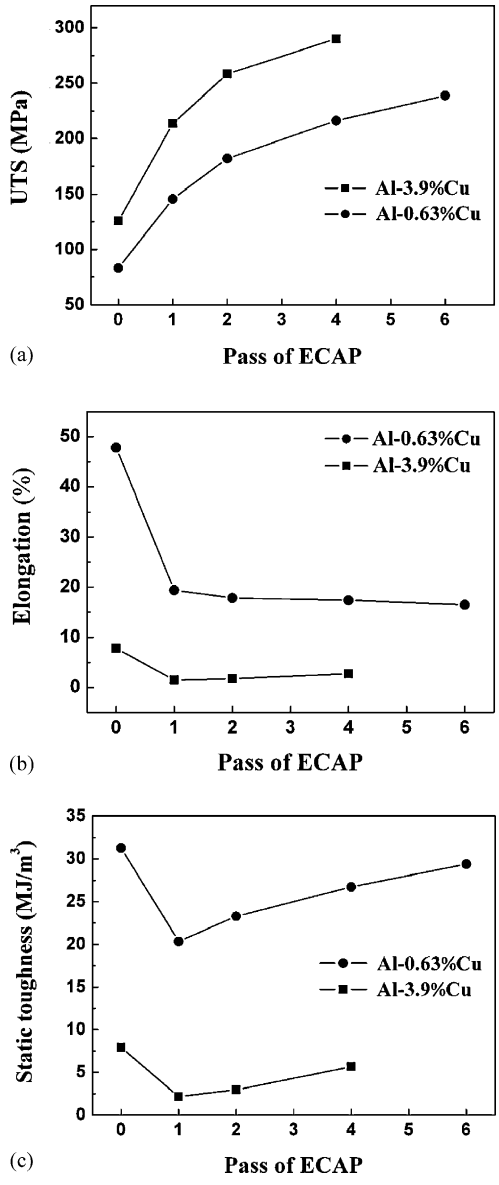

Fig. 8. Dependence of (a) ultimate tensile strength, (b) elongation and (c) static toughness on ECAP pass for Al–0.63% Cu and Al–3.9% Cu alloys.

process. They established a quantitative relationship between the variation of static toughness and the dissipation of cyclic plastic strain energy. However, static toughness was not yet mentioned in the research work studying mechanical properties of the ECAPed materials. Fig. 8(c) shows the variation of static toughness of the two Al–Cu alloys with the passes of ECAP. It can be seen that normally, the master alloys in their casting state have the maximum static toughness, although their UTS is low. It can be explained that their elongation is obviously higher than that of the ECAP state. After one pass, the static toughness obviously decreases though the strength increases, due to a drastic decrease in elongation. Thereafter, the static toughness of the two Al–Cu alloys increases with increasing ECAP passes. When the Al–0.63% Cu alloy was pressed to six passes, its static toughness reaches 30 MJ/m^3, which is quite close to that of the master alloy. This indicates that the strength of the Al–Cu alloy can be obviously improved, while its static toughness is nearly the same as the master alloy without ECAP treatment. It is suggested that ECAP should be a promising method in adjusting the comprehensive mechanical properties among strength, elongation and static toughness of materials.

3.3. Deformation and fracture morphologies

Fig. 9 shows the fracture morphology of the Al–0.63% Cu alloy. The casting specimen exhibits obvious necking before failure, and so is the specimen after one pass, as clearly seen in Fig. 9(a and b). After two passes, the fracture displays a combined feature of shear and necking with a shear angle of about 70° to the load axis (Fig. 9(c)). After four passes, the necking degree decreases clearly, and the shear feature becomes more obvious. The angle between fracture surface and load direction is about 57° (Fig. 9(d)). This means that the shear fracture angle decreases with increasing ECAP passes. The fracture features above indicate that the failure modes of the Al–0.63% Cu alloy change from necking to obvious shear fracture with increasing ECAP passes. This can be explained that the alloy was work-hardened gradually, resulting in a weak necking trend through multiple passes of ECAP treatment.

It can be seen from Fig. 10 that the fracture displays more brittle feature for the Al–3.9% Cu alloy. The failure of the casting sample is fracture normal to the tensile axis, as shown in Fig. 10(a). While after one pass, the fracture becomes shear mode, with a shear angle of about 26°, as marked in Fig. 10(b). This shear fracture surface is approximately paralleled to the streamline direction in Fig. 4(a). With increasing ECAP passes, the Al–3.9% Cu alloy still displays shear fracture mode, and the shear fracture angles gradually decrease to 45°, as marked in Fig. 10(c and d). Thus, the shear fracture surfaces are close to the maximum shear stress plane for the Al–3.9% Cu alloy subjected to two and four passes. This indicates that the shear fracture of the Al–Cu alloy should be mainly controlled by the maximum shear stress and will be discussed in Section 3.4.

3.4. Fracture mechanism

Fig. 11 is the illustration of the fracture mechanisms of the Al–0.63% Cu alloy subjected to different ECAP passes. The casting alloy begins necking down under the tensile stress, and plastic deformation is difficult under the central three-dimensional tensile stress. As a result, the θ phase disengages from the boundary of the matrix, forming micropores which grow continuously and get together to cracks, leading to final fracture. With increasing ECAP pass, the work-hardening degree gradually increases. Thus, though micropores form after necking, it is difficult for the micropores to grow and aggregate, so the shear fracture becomes more predominant under tensile load.

Fig. 12 illustrates the fracture mechanisms of the Al–3.9% Cu alloy with different ECAP passes. There is continuous brittle θ phase distributing along grain boundaries of the casting alloy, which significantly impairs the deformation ability of the grain boundaries. Consequently, the casting Al–3.9% Cu alloy often fails along the grain boundaries under the tensile stress, leading

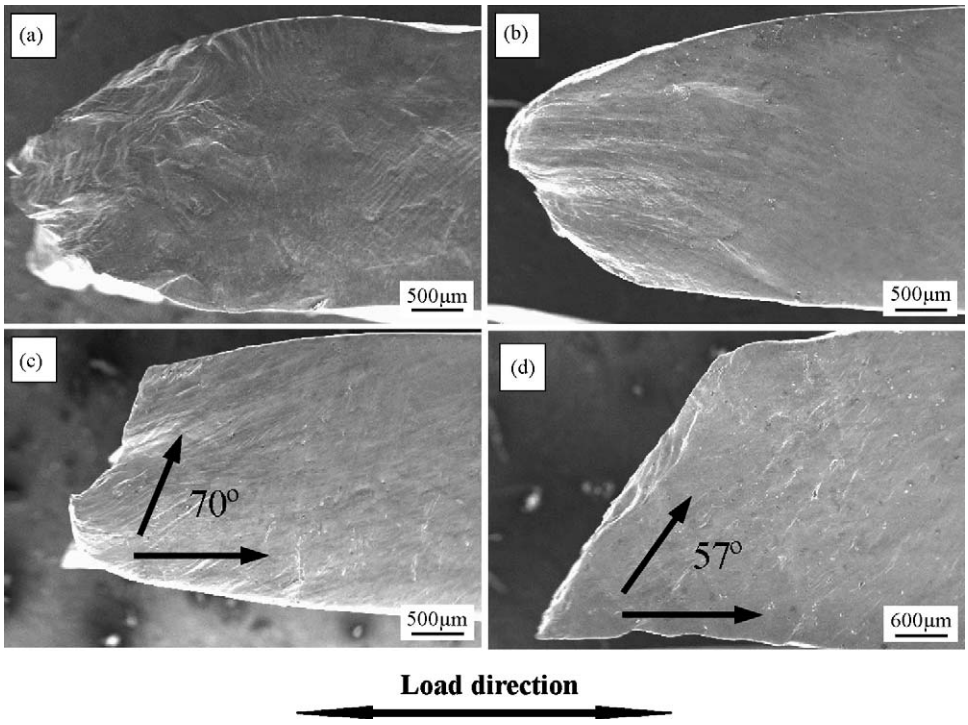

Fig. 9. Fracture morphologies of Al–0.63% Cu alloy (*Y* plane): (a) zero pass, (b) one pass, (c) two passes and (d) four passes.

to a normal fracture (see Fig. 10(a)). After one pass of ECAP, the θ phase distributes mainly along the streamline direction due to intense shearing (see Fig. 4(a and b)). It is supposed that the streamline plane containing the θ phase is the weakest, because the tensile fracture occurs along the plane with a shear angle of about 26° to tensile axis. Before pressed for the second pass, the sample was rotated for 90°, so the streamline plane should be also rotated for 90°. The second pass will cause new streamline different from the first one. Meanwhile, the two streamlines will interact each other during ECAP treatment in the Al–3.9% Cu alloy. Therefore, the microstructure of the Al–3.9% Cu alloy will become more uniform and isotropic with increasing ECAP pass.

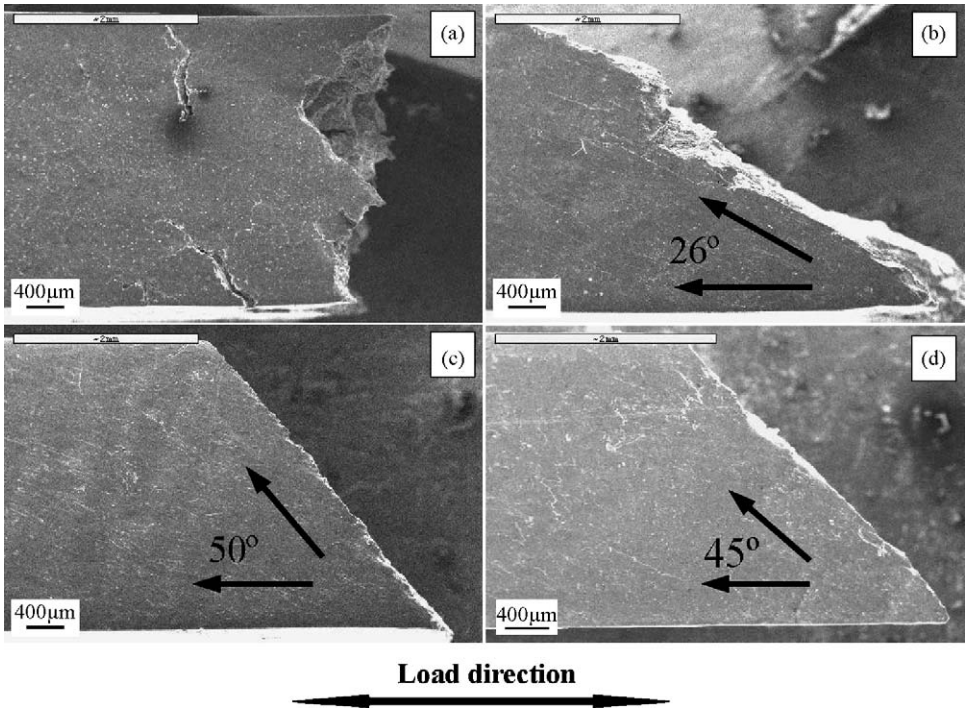

Fig. 10. Fracture morphologies of Al–3.9% Cu alloy (*Y* plane): (a) zero pass, (b) one pass, (c) two passes and (d) four passes.

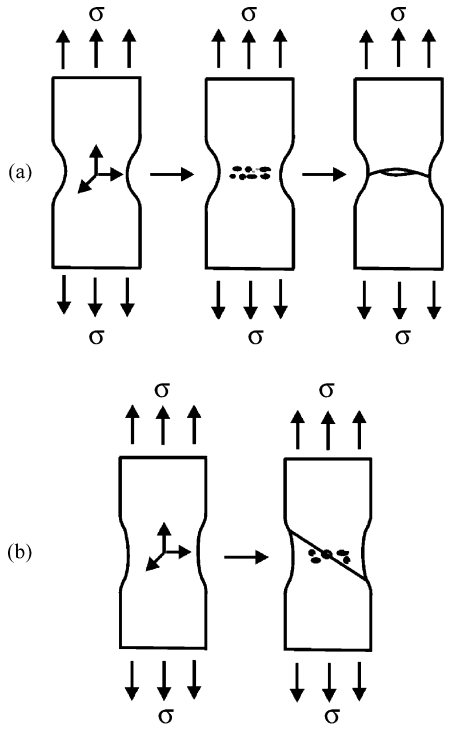

(a) casting state or one pass of ECAP
(b) multiple passes of ECAP

Fig. 11. Illustration of fracture modes for the Al–0.63% Cu alloy with different ECAP passes: casting state or one pass of ECAP multiple passes of ECAP.

After two and four passes, the fracture tends to proceed along the maximum shear stress plane. It can be seen from Fig. 10(c and d) that the shear fracture angles are slightly larger than 45°, which can be attributed to the effect of the normal tensile stress on the shear plane, according to the united tensile fracture criterion [24].

4. Conclusions

Based on the experimental results above, the following conclusions can be drawn:

(1) There appears streamline structure in both of Al–Cu alloys after ECAP treatment. The shear direction makes an angle of about 26° with respect to the longitudinal direction. The grains of Al–Cu alloys are refined to submicron level after four passes of ECAP. In Al–3.9% Cu alloy, the precipitation phase θ along grain boundaries can be broken into disperse nanoscale particles after ECAP treatment.
(2) The tensile strength of Al–0.63% Cu and Al–3.9% Cu alloys has been obviously improved with increasing ECAP pass. However, the elongation of the two alloys maintains almost constant. Therefore, the static toughness of the two alloys was enhanced with increasing ECAP pass.
(3) The failure modes of the two Al–Cu alloys display different features. For Al–0.63% Cu alloy, necking degree decreases clearly, and the shear feature becomes more obvious, with increasing ECAP pass. For Al–3.9% Cu alloy, the failure of the casting sample is fracture normal to the tensile axis. After one pass, shear fracture occurred along the streamline plane, indicating that the streamline plane produced by first pressing is the weakest in Al–3.9% Cu alloy. After two and four passes, the shear fracture tends to proceed along the maximum shear stress plane, indicating a more homogeneous microstructure due to multi-pass ECAP treatment.

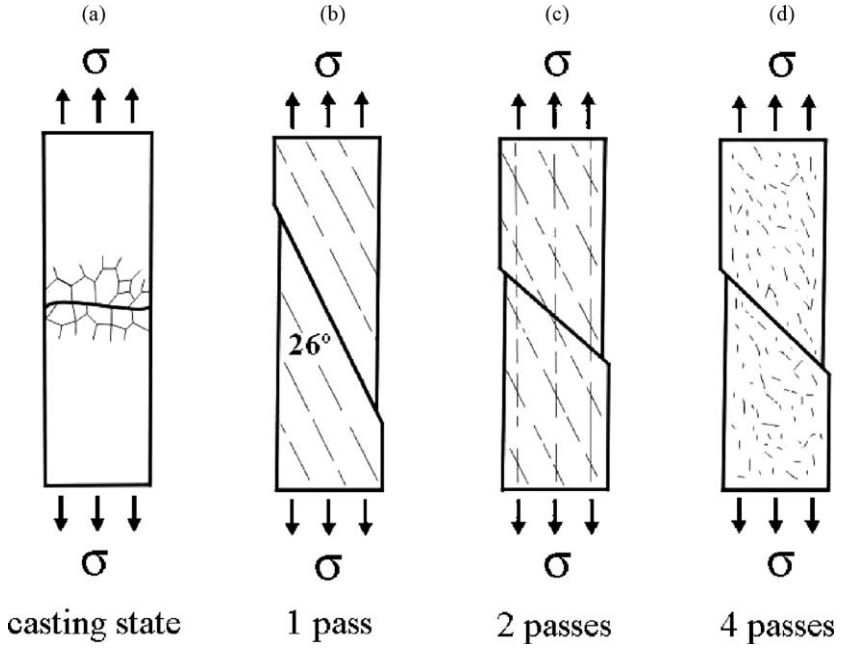

Fig. 12. Illustration of fracture modes for the Al–3.9% Cu alloy with different ECAP passes.

Acknowledgements

The authors would like to thank Gao W., Han W.Z., Su H.H., Wen J.L., Yao G. and Yin S.M. for the assistance in the mechanical tests, SEM observations and stimulating discussions on the manuscript. This work was supported by "Hundred of Talents Project" of the Chinese Academy of Sciences.

References

[1] V.M. Segal, Mater. Sci. Eng. A197 (1995) 157.
[2] V.M. Segal, Mater. Sci. Eng. A271 (1999) 322.
[3] M. Furukawa, Z. Horita, T.G. Langdon, Mater. Sci. Eng. A332 (2002) 97.
[4] M.A. Muñoz-Morris, C.G. Oca, D.G. Morris, Scripta Mater. 48 (2003) 213.
[5] T. Aida, K. Matsuki, Z. Horita, T.G. Langdon, Scripta Mater. 44 (2001) 575.
[6] Z.C. Wang, P.B. Prangnell, Mater. Sci. Eng. A328 (2002) 87.
[7] W.J. Kim, S.I. Hong, Y.S. Kim, S.H. Min, H.T. Jeong, J.D. Lee, Acta Mater. 51 (2003) 3293.
[8] T.L. Tsai, P.L. Sun, P.W. Kao, C.P. Chang, Mater. Sci. Eng. A342 (2003) 144.
[9] M. Murayama, Z. Horita, K. Hono, Acta Mater. 49 (2001) 21.
[10] J.T. Wang, S.B. Kang, H.W. Kim, Mater. Sci. Eng. A383 (2004) 356.
[11] E.J. Zoqui, M.H. Robert, J. Mater. Process. Technol. 78 (1998) 198.
[12] I.J. Polmear, Light Alloys, Edward Arnold, 1981.
[13] M. Furukawa, Y. Iwahashi, Z. Horita, M. Nemoto, T.G. Langdon, Mater. Sci. Eng. A257 (1998) 328.
[14] J. Wang, Y. Iwahashi, Z. Horita, M. Furukawa, M. Nemoto, R.Z. Valiev, T.G. Langdon, Acta Mater. 44 (1996) 2973.
[15] A.D. Shan, I.G. Moon, H.S. Ko, J.W. Park, Scripta Mater. 41 (1999) 353.
[16] A. Gholinia, P. Bate, P.B. Prangnell, Acta Mater. 50 (2002) 2121.
[17] K. Furuno, H. Akamatsu, K. Oh-ishi, M. Furukawa, Z. Horita, T.G. Langdon, Acta Mater. 52 (2004) 2497.
[18] A. Gholinia, P.B. Prangnell, M.V. Markushev, Acta Mater. 48 (2000) 1115.
[19] Z. Horita, T. Fujinami, M. Nemoto, T.G. Langdon, J. Mater. Process. Technol. 117 (2001) 288.
[20] J.Y. Chang, A. Shan, Mater. Sci. Eng. A347 (2003) 165.
[21] W.J. Kim, C.S. Chung, D.S. Ma, S.I. Hong, H.K. Kim, Scripta Mater. 49 (2003) 333.
[22] William D. Callister Jr., Fundamentals of Materials Science and Engineering, fifth ed., John Wiley & Sons Inc., 2001.
[23] D.Y. Ye, Z.L. Wang, Mater. Sci. Eng. A297 (2001) 54.
[24] Z.F. Zhang, J. Eckert, Phys. Rev. Lett. 94 (2005) 094301.